RSC Sustainability

Accepted Manuscript

This article can be cited before page numbers have been issued, to do this please use: J. Honzicek, T. Foltýn, V. Petzný and Š. Podzimmek, *RSC Sustainability*, 2026, DOI: 10.1039/D6SU00297H.

View Article Online
DOI: 10.1039/D6SU00297H

Sustainability spotlight statement. This study presents a practical upcycling strategy for PLA/PLA+ 3D-printing waste, converting it into high-performance, styrene-free polyester resins without extensive purification. The process tolerates complex waste streams and enables room-temperature curing, contributing to circular polymer use and more sustainable materials design.

View Article Online
DOI: 10.1039/D6SU00297H

ARTICLE

Chemical Upcycling of PLA-Based 3D Printing Waste: An Effective Pathway toward Styrene-Free Polyester Resins.

Received 00th January 20xx,
Accepted 00th January 20xx

DOI: 10.1039/x0xx00000x

Jan Honzíček *[a], Tomáš Foltýn,[a] Vojtěch Petzný,[a] Štěpán Podzimek,[a,b]

This study focusses on the valorization of polylactic acid (PLA) waste, including additive-containing materials (PLA+), generated by fused deposition modeling (FDM) 3D printing, which represents a growing environmental concern driven by the increasing adoption of FDM technologies. An efficient chemical upcycling strategy is presenting, enabling the direct transformation of 3D printing waste into value-added, styrene-free unsaturated polyester resins. Thermal depolymerization of PLA using diethylene glycol affords a low-viscosity intermediate, facilitating the efficient removal of fillers and pigments by simple centrifugation or filtration. The generality of the approach was demonstrated across a series of commercial PLA and PLA+ samples. The resulting glycolysate was successfully utilized as a renewable feedstock for the synthesis of itaconate-based polyester with tunable degree of unsaturation. Subsequent formulation with dimethyl itaconate enabled the preparation of room-temperature-curing resins. The optimized system exhibited a high glass transition temperature, good thermal stability, and favorable mechanical performance, including flexural strength of up to 74.9 MPa and a Young's modulus of 2.32 GPa, highlighting the potential of this strategy for the development of sustainable polymer material.

Introduction

Polylactic acid (PLA) is an industrially relevant biobased polyester. Its building block, lactic acid (LA), is produced by fermentation of hexose sugars and oligosaccharides derived from renewable resources such as corn starch, sugarcane, cassava and sugar beet.[1] Although PLA can be synthesized by direct condensation polymerization of LA, it is predominantly produced via ring-opening polymerization of its cyclic diester, known as lactide.[2,3]

PLA is the most widely used bioplastics due to its favorable balance of performance and processability, with an estimated global production capacity estimated to reach ~610 kt in 2025.[3,4] PLA is transparent, food-contact safe, and biodegradable, which supports its widespread use in food packaging and single-use consumer products.[5] It can be processed by conventional techniques such as extrusion, thermoforming, and injection molding and can also be melt-spun into fibers.[6] In addition, PLA is utilized in biomedical applications owing to its biocompatibility and resorbability,[7,8] while its biodegradability is exploited in agricultural and horticultural products.[9] Furthermore, PLA has been explored for separation applications in the development of porous membrane materials.[10]

In recent years, PLA has emerged as a key material for the production of filaments for fused deposition modeling (FDM) 3D printing due to its relatively low melting temperature (T_m = 159–178 °C),[11] ease of processing, low warping tendency, and good dimensional stability. Its limited emission of volatile degradation products, together with broad commercial availability, further contributes to its widespread use in additive manufacturing, particularly in educational, design, and prototyping applications.[12] Despite these advantages, the intrinsic brittleness, relatively low heat resistance, and moderate toughness of neat PLA can limit its performance in functional 3D-printed parts. Consequently, modified PLA grades, commonly referred to as PLA+, as well as PLA-based composites, have been developed to tailor mechanical, thermal, and processing properties. These materials typically incorporate plasticizers, impact modifiers, chain extenders, or reinforcing fillers to address these limitations.[13,14]

As the life cycle of thermoplastic polymers has become a global issue of increasing importance, the end-of-life management of PLA has attracted growing attention.[15,16] Mechanical recycling of PLA has been explored as a resource-efficient option.[17] However, it is most efficient for well-sorted PLA streams with minimal external contamination.[18] In practice, it is primarily applied to postindustrial PLA waste by filament manufacturers, who reprocess off-speciation filaments that do not meet strict quality control standards.[19] The resulting material is commonly referred to as RePLA or RePLA+. Nevertheless, repeated thermal processing can induce chain scission, leading to a reduction in molecular mass and deterioration of mechanical properties.[20,21] These effects are particularly pronounced for filled or blended PLA grades, which exhibit increased sensitivity to thermal degradation.[22]

[a] Institute of Chemistry and Technology of Macromolecular Materials, Faculty of Chemical Technology, University of Pardubice, Studentská 573, 532 10 Pardubice, Czech Republic.
[b] Synpo Ltd, S. K. Neumanna 1316, 532 07 Pardubice, Czech Republic

Electronic Supplementary Information (ESI) available: SEC chromatograms, composition of products, mechanical properties of cured products and testing specimen dimensions. See DOI: 10.1039/x0xx00000x

As an alternative, chemical recycling and upcycling strategies enable the depolymerization of PLA to recover its monomer (*i.e.*, lactide) [23-26] or its precursors, such as lactic acid and methyl lactate.[27-30] These processes typically rely on catalyzed hydrolysis or alcoholysis. Enzymatic hydrolysis of PLA has also been investigated.[31-33] However, such approaches generally suffer from low reaction rates, limited achievable concentrations, and energetically demanding product isolation. Beyond monomer recovery, alternative depolymerization pathways, including alcoholysis,[34-38] aminolysis,[39-41] and reductive depolymerization,[42] enable upcycling PLA waste into higher-value chemicals and functional materials. These strategies offer opportunities to retain or enhance material value and support circular economy concepts for biobased polymers. Nevertheless, their practical implementation is often limited by multistep protocols, tedious purification processes, high energy consumption, the need for expansive catalysts, or low overall yields, which may lead to additional waste generation. Moreover, the range of applications for depolymerization products remains relatively limited, including poly(ester–amide)s [39] and polyurethanes,[43] methacrylate resins,[40] and fumarate-based polyester resins.[44]

In this context, we present a straightforward and efficient upcycling strategy for PLA/PLA+ 3D-printing waste that overcomes these limitations. The process enables direct conversion into a sustainable, styrene-free unsaturated polyester resin without the need for extensive purification. The resulting material performs as a thermosetting resin and constitutes a viable, renewable alternative to conventional general-purpose unsaturated polyester resins derived from fossil feedstocks.

Results and discussion

Characterization of PLA filaments

Eleven PLA samples, including PLA powder (sample **1**) and 3D-printed objects (samples **2–11**) manufactured from commercial PLA/PLA+ filaments of different origins, were selected for depolymerization experiment. All samples were characterized by size-exclusion chromatography (SEC) prior to use.

SEC coupled with multi-angle light scattering (SEC-MALS) confirmed that sample **1** is a high-molar-mass PLA with a unimodal molar mass distribution (M_w = 109 100 g/mol, $Đ$ = 1.42), suitable for industrial applications.[45] Comparative analysis using the more commonly used SEC with a refractive index detector (SEC-RI), calibrated against polystyrene standards, yielded significantly higher values of apparent molar mass values for PLA. In this case, M_w and $Đ$ were overestimated by factors of 1.75 and 1.6, respectively, relative to the absolute values obtained by SEC-MALS (Table 1).

Filament-derived samples (**2–11**) were analyzed by SEC-RI. Although less informative, this method allows comparison with sample **1** under the assumption of similar chemical composition and macromolecule architecture.

Samples **2**, **3**, **10** and **11** exhibited unimodal molar mass distributions comparable to that of sample **1**, with similar M_w and $Đ$ values (Table 1). In contrast, samples **4–9** displayed broader molar mass distributions, reflected in higher dispersities and lower M_w values. This behavior suggests the presence of blended systems comprising high- and medium-molar-mass PLA fractions, likely introduced to achieve a targeted viscosity window and ensure consistent processing performance. This interpretation is further supported by the SEC traces, which show either a second maximum or a pronounced shoulder at higher elution times (see Figures S4–S9 in the Supporting Information).

Table 1. Molar mass distribution of PLA/PLA+ samples determined by SEC

Sample	Method	M_n (g/mol) [a]	M_w (g/mol) [b]	$Đ$ [c]
1	SEC-MALS	77 000	109 100	1.42
1	SEC-RI	84 000	190 700	2.27
2	SEC-RI	80 300	186 700	2.33
3	SEC-RI	85 400	202 300	2.37
4	SEC-RI	41 300	166 600	4.03
5	SEC-RI	40 400	165 500	4.10
6	SEC-RI	23 200	134 200	5.78
7	SEC-RI	29 700	145 200	4.88
8	SEC-RI	33 000	142 000	4.31
9	SEC-RI	36 600	162 500	4.44
10	SEC-RI	64 400	171 900	2.67
11	SEC-RI	70 100	163 400	2.33

[a] Number-average molar mass. [b] Weight-average molar mass. [c] Dispersity.

Glycolysis of PLA samples

Thermal depolymerization of PLA powder (sample **1**) in the presence of one molar equivalent of diethylene glycol (DEG; calculated on repeating unit of PLA; M_r = 72.06 g/mol) at 240°C for 2h afforded a pale yellow solution containing a minor amount of white wax (0.41 wt.% based in PLA). The solid impurity was removed by centrifugation and identified by IR spectroscopy as a mixture of a polyester resin and a polyamide (see Figure 26 in the Supporting Information).

Preliminary optimization experiments revealed that reaction times shorter than 30 min resulted in incomplete depolymerization. The process was intentionally performed under catalyst-free conditions to simplify the overall upcycling protocol. As glycolysis reactions of polyesters can be efficiently catalyzed by zinc acetate [46] and metal-containing ionic liquids,[47] further optimization through catalyst-assisted depolymerization represents a promising route toward reducing the energy demand of the process.

The ^{1}H NMR spectrum of the crude product revealed diethylene glycol monolactate (LA-DEG) as the major component (65%), accompanied with DEG (25%) and minor byproducts, including lactide (5%) and diethylene glycol dilactate (LA-DEG-LA; 5%); see Figure 1. Pure LA-DEG was subsequently isolated by vacuum distillation and characterized by ^{1}H and ^{13}C-APT NMR spectra (Figures 14 and 15 in the Supporting information).

The high selectivity toward LA-DEG formation, achieved without the use of excess DEG, is ascribed to the lower thermodynamic stability of ester linkages involving secondary hydroxyl group. This behavior contrasts with that of poly(ethylene

View Article Online
DOI: 10.1039/D5SU00397H

terephthalate) (PET) [48] and poly(ethylene-2,5-furanoate) (PEF),[49] for which more complex product mixtures containing higher oligomers are typically formed under comparable conditions.

Depolymerization of PLA objects (samples **2**–**11**), printed from commercial PLA/PLA+ filaments using the same PLA-sample/DEG ratio as in the case of sample **1** (*w*/*w*), resulted in suspensions of varying appearance (Figure 2) due to presence of colorants, pigments, fillers, and other additives. Nevertheless, in all cases, the liquid phase obtained after centrifugation exhibited similar composition, as confirmed by ^{1}H NMR spectroscopy.

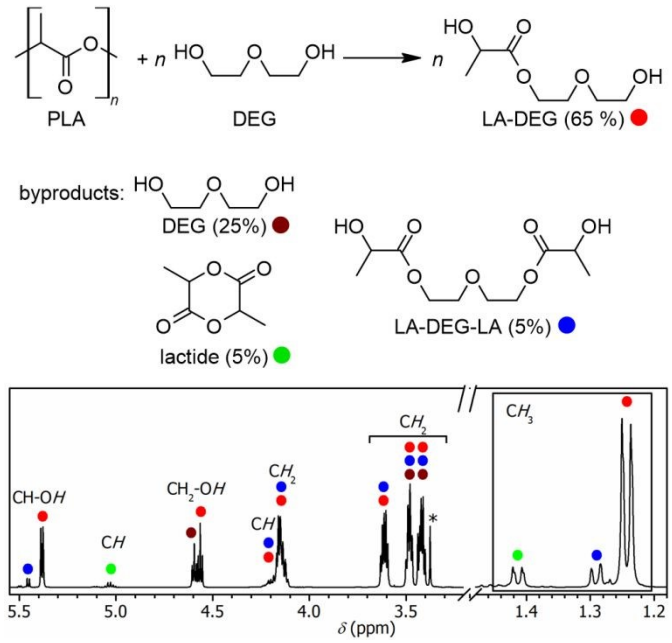

Figure 1. Glycolysis of PLA by one equivalent of DEG with assignment of the ^{1}H NMR spectrum of the reaction product.

The main variation was observed for samples **4**–**10**, which displayed minor signals at 8.04 and 2.28 ppm in the ^{1}H NMR spectra, indicating the presence of glycolyzed poly(butylene adipate-*co*-terephthalate) (PBAT), a common additive in commercial PLA filament formulations. Its content was established to be in the range of 3–5 wt.% (relative to PLA polymer) for samples **4**, **5**, **7**–**9**, while higher amounts were detected in sample **6** (8 wt.%) and sample **10** (12 wt.%).

The amount of solid residues in the glycolyzed samples **2**–**11** varied from 0.04 to 9.15 wt.% (Figure 2). Their composition was qualitatively analyzed by infrared spectroscopy. In sample **2**, the solid fraction (upper phase) consisted of an acrylic resin. A broad absorption band below 600 cm^{-1} observed in samples **3**–**6** and **8**, indicates the presence of inorganic pigments. Characteristic bands at 3299, 2915, 2848, 1634, and 1554 cm^{-1} reveal the presence of polyamide 66 in the samples **3**–**6** and **9**. In sample **7**, the solid fraction (upper phase) was identified as a polystyrene-based masterbatch. Samples **10** and **11** contained carbon black in combination with carbonates (1417 cm^{-1}) and silicates (1003 and 3676 cm^{-1}).

For a more detailed investigation, sample **10** was selected as a representative of objects printed from a filled PLA+ filament, declared by the supplier to be recycled from technological waste (RePLA+). The glycolysis procedure was scaled up to enable processing of 100 g of PLA objects in a single batch. Key modifications included removal of inorganic pigments and fillers by hot filtration using a Büchner funnel and reduction of the DEG amount to increase the LA-DEG content in the glycolysate. Notably, the resulting product exhibited low viscosity at room temperature (0.11 Pa·s), which facilitated handling and efficient filtration. Using an adjusted molar ratio of PLA to DEG of 54:46 (accounting for the filler content), the glycolysate contained an increased fraction of LA-DEG (76%) and a reduced amount of DEG (14%). Minor byproducts, including lactide (5%) and LA-DEG-LA (5%) were present in amounts comparable to those observed for the sample 1. The resulting crude product was obtained in 95% yield and was subsequently used for the preparation of unsaturated polyester without other purification.

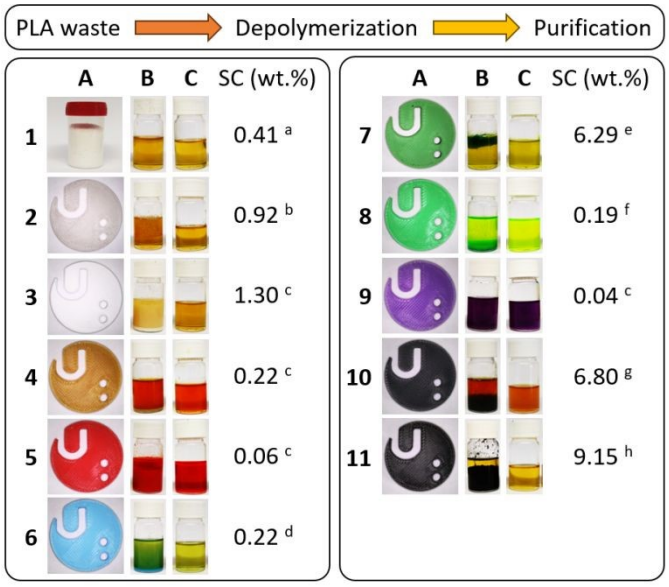

Figure 2. Depolymerization of PLA. A) Depolymerized specimen, B) crude product of glycolysis, C) product purified by centrifugation, SC) solid content in crude product expressed relative to initial weight of PLA specimen. Appearance of solid content after washing and drying: a) white wax, b) colorless film, c) white powder, d) blue powder, e) blue solid, f) green solid, g) black powder, h) black film.

Synthesis of itaconate-based polyesters

The depolymerized product obtained from samples **10**, containing LA-DEG as the major component, was utilized as a feedstock for the synthesis of itaconate-based polyesters. These binders were prepared via condensation polymerization with itaconic anhydride (IAn) and additional DEG in toluene. Three polyester binders with varying degrees of unsaturation were designed by adjusting the feed composition (Table 2).

The reactions were carried out in the presence of *p*-toluenesulfonic acid and dibutyltin oxide as catalysts at temperatures not exceeding 160°C to minimize the risk of itaconate isomerization.[49] The water formed during the reaction was continuously removed using a Dean-Stark apparatus, and the reaction was terminated once the acid number decreased below 30 mg KOH/g.

View Article Online
DOI: 10.1039/D5SU00267H

The resulting polyester binders UPLA-1 and UPLA-2 exhibited weight-average molar masses (M_w) of 2200 and 1800 g/mol and dispersities ($Đ$) of 2.3 and 2.4, respectively, as determined by SEC-MALS. The molar mass distributions of UPLA-3 is shifted toward higher molar masses, as evident from the distribution curves shown in Figure 3. The higher M_w value (5 900 g/mol) is likely associated with the lower content of secondary hydroxyl functionalities in the feed (Table 2), which favors the chain growth. The markedly higher value of M_z value (288 000 g/mol) for UPLA 3 corresponds to the presence of a small fraction with molar mass up to ~ 10^6 g/mol.

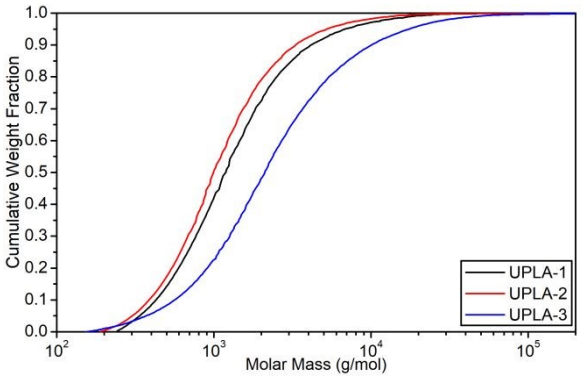

Figure 3. Cumulative molar mass distribution of PLA polyesters.

Infrared spectra of the neat binders confirmed the presence of unsaturated itaconate segments ($\nu_{C=C}$ = 1638 cm^{-1}) [50] and the polyester backbone ($\nu_{C=O}$ = 1718 cm^{-1}), as shown in Figures S40–S43 in the Supporting Information.

^{1}H NMR spectroscopy confirmed the incorporation of the expected building blocks and enabled their quantification. The overall content of LA segments was consistent with the feed compositions across the series, as indicated by the integral intensities of the LA methyl signals observed at 1.38–1.53 ppm (Figure 4). The chemical shift of the methine (CH) group allowed differentiation between LA units incorporated into the polyester backbone (δ = 5.12 ppm) and those bearing unesterified hydroxyl groups at the chain termini (δ = 3.56 ppm). The higher fraction of terminal LA units (69.0–77.6 %) is attributed to the lower reactivity of the secondary hydroxyl group of LA compared to the primary hydroxyl group of DEG.

Table 2. Properties of synthesized UPLA polyesters.

Polyester	UPLA-1	UPLA-2	UPLA-3
Feed composition (mol. %)			
LA-DEG [a]	31.0/26.5	24.1/20.7	19.8/16.9
IA	28.3	33.1	36.2
DEG	14.2	22.1	27.1
Actual composition (mol. %) [b]			
LA	30.3 (20.9)	22.7(16.6)	18.2(14.1)
IA	27.4	32.9	34.6
MES	0.4	0.5	0.6
TPA	0.6	0.5	0.4
ADA	0.8	0.7	0.4
DEG	36.3	39.9	41.7
TTEG	4.2	2.8	4.2
Polyester properties			
AV (mg KOH/g)	28	27	7
M_n (g/mol) [c,d]	900	800	1 300
M_w (g/mol) [d,e]	2 200	1 800	5 900
M_z (g/mol) [d,f]	15 000	9 000	288 000
$Đ$ [d,g]	2.4	2.3	4.6
Viscosity (Pa·s)	14.1	16.1	42.1

[a] LA segments / DEG segments in glycolyzed sample **10**. [b] Determined by ^{1}H NMR spectroscopy. [c] Number-average molar mass. [d] Determined by SEC-MALS. [e] Weight-average molar mass. [f] Z-average molar mass. [g] Dispersity.

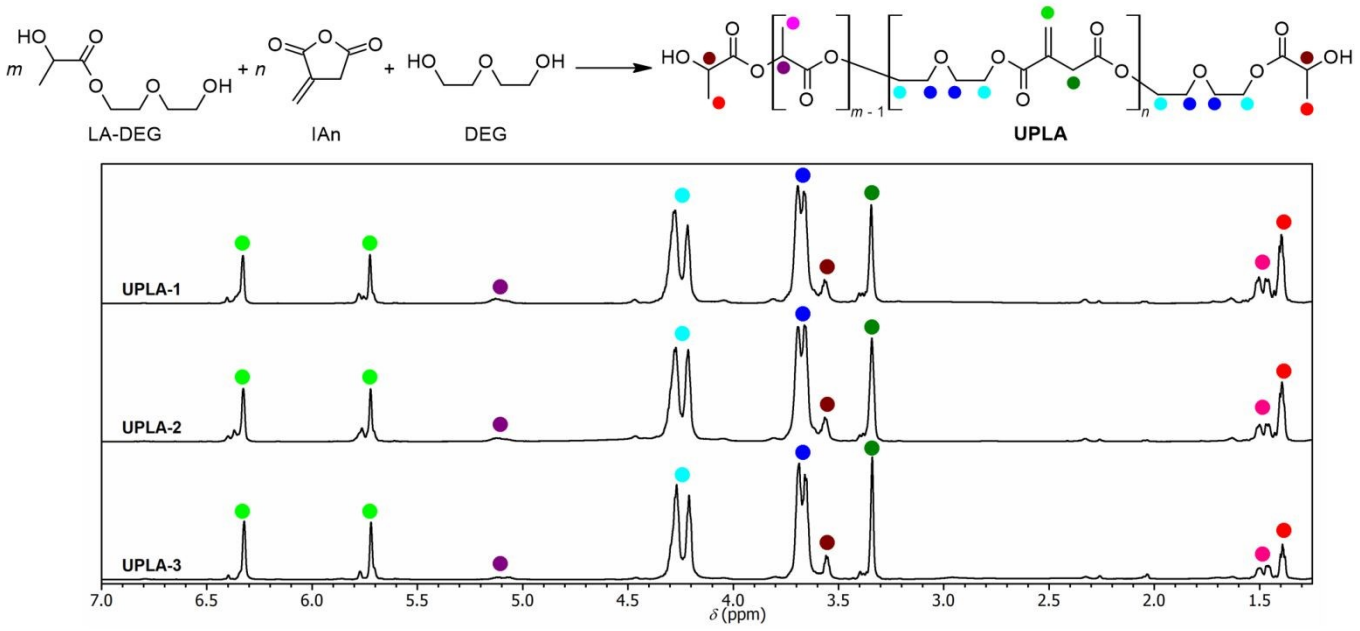

Figure 4. Synthesis of UPLA polyesters and assignment of their ^{1}H NMR spectra to the main building blocks.

View Article Online
DOI: 10.1039/D6SU00297H

ARTICLE

The NMR data further confirmed that itaconic anhydride predominantly forms itaconate (IA) segments with minimal isomerization to mesaconate (MES), with less than 2% conversion observed. DEG-derived segments exhibited signals at 4.19–4.33 and 3.62–3.74 ppm, corresponding to methylene groups adjacent to ester and ether functionalities, respectively. The higher intensity of the later signal indicates partial dimerization of DEG to tetraethylene glycol (TTEG) during the synthesis. Integration of these signals revealed that 18.7%, 12.3%, and 16.8% of DEG was converted to TTEG units in binders UPLA-1, UPLA-2 and UPLA-3, respectively. Additionally, minor terephthalate (TPA) and adipate (ADA) units were detected by NMR spectroscopy, originating from glycolyzed PBAT additives present in the sample **10**.

The prepared binders were liquid at room temperature, with dynamic viscosity of 14.1 and 16.1 Pa·s for UPLA-1 and UPLA-2, respectively. A significantly higher viscosity was observed for UPLA-3 (42.1 Pa·s), which is attributed to its higher molar mass. To meet the requirements for general-purpose, room-temperature-curing resins, the formulations were diluted with dimethyl itaconate (DMI), selected for its low volatility and accessibility from renewable resources. In addition, DMI is expected to introduce rigid segments into the cured polyester network, thereby contributing to an increase in the glass transition temperature (T_g).

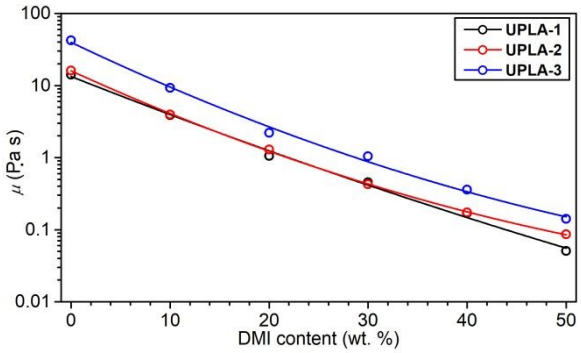

Figure 5. Effect of DMI content on dynamic viscosity of UPLA formulations.

The data presented in Figure 5 illustrate the effect of reactive diluent content on the viscosity, which decreases with increasing DMI concentration. A content of 40 wt.% was selected for further experiments, as it reduced viscosity of all binders below 1 Pa·s. To further investigate the influence of reactive diluent concentration in a system with a high degree of unsaturation, an additional formulation of UPLA-3 containing 20 wt.% DMI (UPLA-3_DMI20) was prepared.

The polyester resins were cured at room temperature using a redox initiation system consisting of butanone peroxide (MEKP) as the initiator and oxidovanadium(IV) dibutylphosphate as the accelerator.[51] After 24 h, the resulting hard, rigid specimens were post-cured at 50, 100 and 150 °C. Infrared spectroscopy indicated ~90% conversion of the C=C double bonds, as evidenced by the decrease in the intensity of the characteristic band at 1638 cm^{-1} ($\nu_{C=C}$).

The gel content of the final materials was determined by extraction with THF (Table 3). A relatively low gel content obtained for formulation UPLA-1_DMI40 (92.1%) indicates a presence of a significant fraction of uncrosslinked polymer. This behavior is attributed to an insufficient concentration of IA segments bearing polymerizable double bonds in the polyester backbone. As the molar mass of UPLA-1 did not reach the values previously obtained for FDCA-based polyesters,[51] a higher content of IA is required to achieve satisfactory crosslinking. Consequently, formulations based on UPLA-2 and UPLA-3 exhibited gel contents above 98%, which are typical for itaconate-based resins [52] and indicate the formation of a well-crosslinked polymer network.

Dynamic mechanical analysis (DMA) revealed that increasing the content of itaconate (IA) and DEG segments in the polyester backbone leads to an increase in the glass transition temperature (T_g). The T_g values increased in the order: UPLA-1_DMI40 < UPLA-2_DMI40 < UPLA-3_DMI40, in parallel with the increasing crosslink density (ν_e) calculated from the storage modulus in the rubbery region (G'_0); see Figure 6 and Table 3. This trend indicates that the effect of increased crosslink density outweighs the plasticizing influence of the flexible DEG units incorporated into the polymer backbone. In addition, the higher molar mass of UPLA-3, discussed above, further contributes to the increased T_g and ν_e values observed for its formulation.

For the formulation with lower DMI content (UPLA-3_20DMI), the material lost its mechanical integrity at elevated temperatures, with sample rupture occurring at ~95 °C. Consequently, the determination of G'_0, required for the calculation of ν_e, was not feasible. Nevertheless, the lower maximum on the loss factor (tan δ) curve indicates reduced energy dissipation and a more elastic network response. This behavior is commonly associated with a higher network density and is consistent with the higher concentration of C=C double bonds in the polyester backbone relative to DMI. The lower T_g value (79.5°C) is therefore attributed to the reduced content of rigid DMI segments in the cured network.

View Article Online
DOI: 10.1039/D6SU00287H

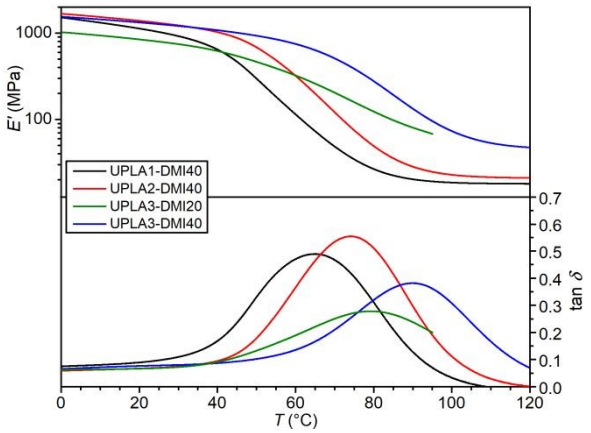

Figure 6. DMA curves of cured UPLA formulations.

Thermogravimetric analysis (TGA) demonstrated that all cured UPLA resins are thermally stable above 200 °C. The temperature corresponding to 5% weight loss ($T_{5\%}$) increased in the order: UPLA-1_DMI40 < UPLA-2_DMI40 < UPLA-3_DMI40 < UPLA-3_DMI20, reflecting the increasing crosslink density of the polymeric network. All formulations exhibited similar TGA profiles, characterized by a single major degradation step in the temperature range of approximately 300–450 °C. The residual mass at the end of the experiment (Char) ranged from 14.6 to 17.1%, indicating comparable char yields among the investigated resins (Figures S48–51 in the Supporting Information).

Mechanical properties of the cured resins were evaluated by flexural testing, with representative stress-strain curves shown in Figure 7. The ultimate flexural stress ($\sigma_{f,max}$) and Young's modulus (E_f) increased in the order: UPLA-1_DMI40 < UPLA-2_DMI40 < UPLA-3_DMI40, consistent with the higher IA content corresponding increase in crosslink density, as evidenced by DMA. This enhancement in stiffness and strength was accompanied by reduced flexibility, as indicated by a decrease in strain at break ($\varepsilon_{f,failure}$) and increasing brittleness. In contrast, the formulation with lower DMI content (UPLA-3_DMI20) exhibited inferior mechanical performance, with reduced flexural strength, modulus, and flexibility compared to UPLA-3_DMI40.

Table 3. Mechanical properties of cured UPLA resins.

	Gel[a] (wt.%)	T_g[b] (°C)	v_e[c] (mmol/cm³)	$\sigma_{f,max}$[d] (MPa)	E_f[e] (GPa)	$\varepsilon_{f,failure}$[f] (%)	$T_{5\%}$[g] (°C)	Char[h] (%)
UPLA-1_DMI40	92.1	65.3	5.82	38.0 ± 1.9	1.21 ± 0.07	5.2 ± 0.8	235.6	15.6
UPLA-2_DMI40	98.2	74.2	6.60	66.1 ± 4.5	1.91 ± 0.11	4.6 ± 0.3	254.2	17.1
UPLA-3_DMI20	98.3	79.5	–	57.1 ± 7.4	2.02 ± 0.20	3.5 ± 0.7	284.0	16.1
UPLA-3_DMI40	98.9	90.1	13.68	74.9 ± 6.6	2.32 ± 0.13	3.8 ± 0.7	271.2	14.6

[a] Gel content. [b] Temperature of glass transition determined by DMA analysis as maximum of the *tan* δ peak. [c] Cross-link density. [d] Ultimate flexural strength. [e] Flexural modulus. [f] Flexural strain at break. [g] Temperature at 5% mass loss in the nitrogen atmosphere from TGA. [h] Char yield from TGA.

The most promising material, UPLA-3_DMI40, exhibited a high ultimate flexural stress (74.9 ± 6.6 MPa) and a Young's modulus of 2.32 ± 0.13 GPa. Notably, these properties are achieved despite absence of rigid aromatic segments in the polyester backbone, which are typically associated with enhance mechanical performance through intermolecular interactions.[48,51,52]

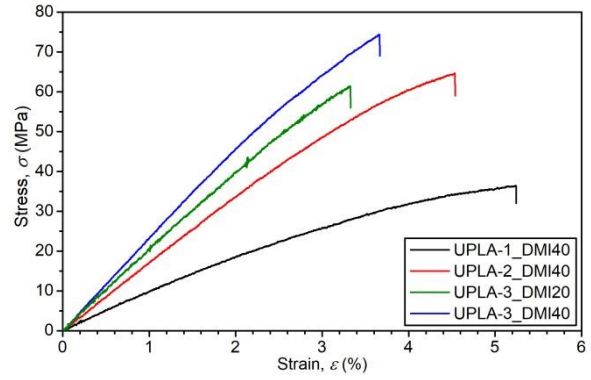

Figure 7. Stress-strain curves of UPLA formulations.

This study presents an effective strategy for the valorization of waste derived from 3D-printed PLA/PLA+ filaments, with an emphasis on minimizing reaction and purification steps. Glycolysis using DEG affords a low-viscosity product containing LA–DEG as the main component, enabling efficient removal of fillers and additives by simple filtration. The robustness and generality of this approach were demonstrated across ten samples of 3D-printed objects originating from diverse PLA sources.

On a representative PLA+ sample, the glycolysis process was successfully scaled up and optimized, and its applicability was demonstrated through the synthesis of unsaturated polyester resin suitable for styrene-free formulations. The optimized system, comprising a polyester with ~34.6 % itaconate segments in the backbone and 40 wt. % of an itaconate-based reactive diluent, exhibited a high glass transition temperature, good thermal stability, and favorable mechanical properties (Figure 8). Overall, this approach establishes a practical and efficient upcycling strategy for the transformation of PLA/PLA+ waste into room-temperature-curing resin systems, providing viable pathway toward transition to a circular economy.

Conclusions

View Article Online
DOI: 10.1039/D5SU00207H

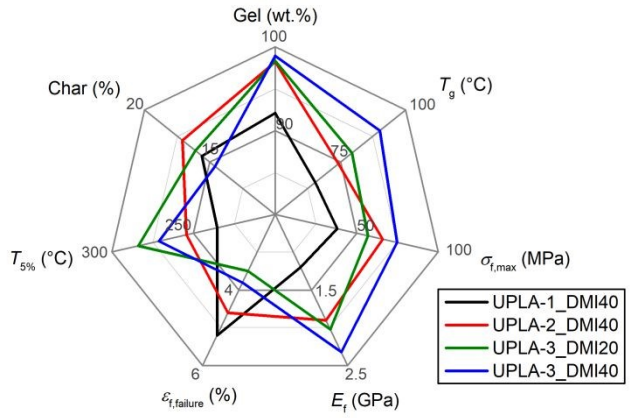

Figure 8. Overview of mechanical properties of cured UPLA resins.

Experimental Section

Materials

Dimethyl itaconate (DMI) and itaconic anhydride (IAn) were supplied from BLDPharmatech. Hydroquinone and *p*-toluenesulfonic acid monohydrate (TsOH) were obtained from Thermo Fisher Scientific. Diethylene glycol (DEG), and tetrahydrofuran (THF) were purchased from Penta and toluene from Lach-Ner. Dibutyltin oxide (DBTO) was obtained from PMC Group. Butanone peroxide (MEKP; 32% in a mixture of dimethyl phthalate and dicetone alcohol) was supplied from Stachema. Oxidovanadium(IV) dibutylphosphate (10.6% V) was synthesized according to previously reported procedure.[51]
PLA materials were obtained from various commercial sources. PLA powder (sample **1**) was supplied by Suntechem. Filament samples (**2**–**11**, diameter 1.75 mm) included: natural transparent filament (**2**, Verbatim), traffic white Extrafill filament (**3**, Fillamentum), gold (**4**), green (**8**), and purple (**9**) filaments (C-TECH), red (**5**), sky blue (**6**), and green (**7**) filaments (Gembird), RePLA+ recycled filament (**10**, Filament PM), and black filament (**11**, Elegoo).

3D printing of the PLA objects

Printing was performed on an FDM Centauri Carbon 3D printer (Shenzhen Elegoo Technology). Prints were prepared using the ElegooSlicer software with the following parameters: nozzle temperature 210°C; bed temperature 60°C; default printing speed for generic PLA and a layer height of 0.2 mm. The infill pattern was set to gyroid with a density of 70%, resulting in printed objects with a mass of ~2g.

Glycolysis of PLA samples

A mixture of three PLA (6.0 g) and DEG (8.8 g) was heated to 240 °C and stirred (300 rpm, PTFE-coated magnetic stirring bar) for 2 h under a nitrogen atmosphere. After cooling to room temperature, the resulting suspension was centrifugated to separate a clear liquid phase. The content of the solid fraction was determined after washing with acetone and vacuum drying. This procedure was applied to each PLA sample.

For scale-up, a modified procedure was employed for sample **10**. A mixture of PLA (100.0 g) and DEG (117.6 g) was heated to 240 °C and stirred (300 rpm) for 2 h under a nitrogen atmosphere. The resulting suspension was filtered while hot under reduced pressure using a Büchner funnel to remove insoluble components. The obtained homogenous glycolysate was used directly for polyester synthesis without further purification.

Synthesis of polyester UPLA-1

PLA glycolysate (30.0 g), IAn (18.9 g), DEG (9.0 g), TsOH (0.12 g), hydroquinone (25 mg) and DBTO (0.49 g) were charged into a reaction vessel and heated to 160°C under a nitrogen atmosphere. Toluene was added to enable azeotropic removal of water while maintaining the temperature below 160 °C. The water formed during the polyesterification was continuously removed using a Dean-Stark apparatus. The reaction progress was monitored by acid value determination and terminated when the acid value decreased below 30 mg KOH/g. Toluene was subsequently removed under reduced pressure at 160 °C. The resulting orange liquid was then discharged and stored at low temperature.

Synthesis of polyester UPLA-2

The reaction was carried out as described for UPLA-1 using PLA glycolysate (30.0 g), IAn (28.3 g), DEG (18.0 g), TsOH (0.19 g), hydroquinone (38 mg) and DBTO (0.76 g).

Synthesis of polyester UPLA-3

The reaction was carried out as described for UPLA-1 using with PLA glycolysate (30.0 g), IAn (37.8 g), DEG (26.8 g), TsOH (0.20 g), hydroquinone (40 mg) and DBTO (0.80 g).

Preparation of test specimens

A mixture of UPLA polyester and DMI (total mass 13 g) was combined with oxidovanadium(IV) dibutylphosphate (50 mg) and stirred until a homogenous formulation was obtained. MEKP (55 µL) was then added, and the mixture was briefly stirred and then centrifuged (6000 rpm, 2 min) to remove entrapped air. The formulation was subsequently poured into silicone molds and allowed to cure at room temperature overnight. Post-curing was carried out in an oven at 50°C for 1 h, 100°C for 1 h, and 150°C for 1 h, followed by colling to room temperature in the closed oven. The resulting specimens were cuboids with dimensions of 50 × 6 × 3 mm^3.

Gel content

Cured specimens of respective resin were ground in an impact mill IKA A10 Basic under liquid nitrogen cooling. The resultim powder (~1 g) was accurately weighted (m_1), suspended in THF (30 mL) and stirred in a sealed Erlenmeyer flask overnight. The insoluble fraction was then collected by filtration, dried in an oven at 50 °C overnight, and weighted (m_2). The gel content (%) was calculated according to Eq. 1:

$$\mathbf{GEL} = \frac{\boldsymbol{m_2}}{\boldsymbol{m_1}} \times \mathbf{100} \quad (1)$$

NMR spectroscopy

^{1}H NMR and ^{13}C APT spectra were recorded on Bruker Avance 400 and 500 MHz spectrometers at room temperature using $CDCl_3$ or DMSO-d^6 as solvents. Chemical shifts (δ) are reported in ppm relative to tetramethylsilane (δ = 0), with calibration performed using the residual signals of the undeuterated solvents.

Infrared spectroscopy

Infrared spectra were recorded on a Nicolet iS50 FTIR spectrometer (Thermo Fisher Scientific) equipped with a diamond ATR crystal over the range of 4000–400 cm^{-1} with a data spacing of 0.5 cm^{-1}. The conversion of UPLA formulations was determined by integrations of the C=C stretching band at 1638 cm^{-1} using a fixed two-point baseline (1620–1655 cm^{-1}). The spectra were normalized to the C=O stretching band integrated over the range 1660–1800 cm^{-1}.

Size exclusion chromatography

Molar mass distributions of PLA filaments were determined using a Waters Alliance e2695 system equipped with a refractive index detector 2414 and two Agilent Mixed-C columns (300 × 7.5 mm^2) using chloroform as the mobile phase (1 mL/min). Samples were dissolved in chloroform (c = 3 mg/mL), filtered through 0.45 µm filters and analyze using an injected volume of 100 µL. Calibration was performed using polystyrene standards covering a molar mass range of 162 to 6 × 10^6 g/mol. Absolute molar mass distributions were determined by SEC coupled with multi-angle light scattering (SEC-MALS) using an Agilent 1200 Series system equipped with an isocratic pump and an autosampler, coupled with a Wyatt HELEOS MALS detector and Optilab T-rEX refractive index detector. Separation was caried out on two Agilent Mixed-C columns (300 × 7.5 mm^2) using tetrahydrofuran (THF) as the mobile phase at a flow rate of 1 mL/min. Samples were prepared in THF at a concentration of ~15 mg/mL and filtered prior use; the injected volume was 100 µL. PLA sample **1** was additionally analyses under SEC-MALS conditions in chloroform using the same setup.

Dynamic Mechanical Analysis

Measurements were performed using a DMA303 Eplexor instrument (Netzsch) in single-cantilever configuration (clamp span 11 mm, displacement amplitude ±0.15 mm, frequency 1 Hz). The temperature range was −60 to 160 °C at a heating rate of 3°C/min. The glass transition temperature (T_g) was determined from the maximum on the loss factor (tan δ) curve. The crosslink density (v_e) was calculated using Eq. 2:

$$v_e = \frac{G'_0}{R \times T} \quad (2)$$

where G'_0 is the storage modulus in the rubbery plateau (taken at $T = T_g + 50$ K), R is the universal gas constant, and T is the absolute temperature in kelvin.

Thermogravimetric analysis

TGA analyses were carried out using a STA 449 F5 Jupiter instrument (Netzsch) equipped with a TG holder. Analyses were performed under a nitrogen atmosphere over the temperature range of 30–550 °C at a heat rate of 10 °C/min and a nitrogen flow rate of 50 mL/min. Samples (~10 mg) were analyzed in the form of compact specimens.

Viscosity

Dynamic viscosities (µ) were measured using a Malvern Kinexus rotational rheometer equipped with a Peltier plate geometry (gap 0.2 mm). Measurements were performed at 25 °C with the shear rate increased stepwise from 0.1 to 100 s^{-1} in 16 increments to assess potential non-Newtonian behavior.

Mechanical testing

Flexural properties were evaluated using a universal testing machine Autograph AGS-X 50kN (Shimadzu) in a three-point bending configuration with a support span of 40 mm at a crosshead speed of 1 mm/min. The test was terminated upon specimen rupture or when the applied force dropped below 10 N.

Author Contributions

J.H. conceptualized the project, interpreted NMR data, performed IR experiments, wrote the original manuscript, and edited the manuscript. T.F. contributed to the reaction experiments. V.P. performed all reaction experiments and characterized materials. Š.P. performed SEC experiments.

Conflicts of interest

There are no conflicts to declare.

Acknowledgements

The authors are grateful for the financial support from The Ministry of Education, Youth and Sport of the Czech Republic (Project No. SG362005) and to prof. Libor Dostál for NMR spectra acquisition.

Notes and references

1 M. Dusselier, P. Van Wouwe, A. Dewaele, E. Makshina, B. F. Sels, *Energy Environ. Sci.*, 2013, **6**, 1415–1442. https://doi.org/10.1039/c3ee00069a
2 J. Yu, S. Xu, B. Liu, H. Wang, F. Qiao, X. Ren, Q. Wei, *Eur. Polym. J.*, 2023, **193**, 112076. https://doi.org/10.1016/j.eurpolymj.2023.112076
3 C. Shi, E. C. Quinn, W. T. Diment, E. Y.-X. Chen, *Chem. Rev.*, 2024, **124**, 4393–4478. https://doi.org/10.1021/acs.chemrev.3c00848
4 European Bioplactics e.V., Bioplastics Market Development Update 2025, 2025, https://www.european-bioplastics.org/bioplastics-market-development-update-2025/, Accessed 15th May 2026.
5 T. A. Swetha, A. Bora, K. Mohanrasu, P. Balaji, R. Raja, K. Ponnuchamy, G. Muthusamy, A. Arun, *Int. J. Biol. Macromol.*,

2023, **234**, 123715. https://doi.org/10.1016/j.ijbiomac.2023.123715

6 X. Li, A. Farooq, M. Hua, Y. Pan, P. Yu, M. Jian, L. Yao, C. Gao, G. Pan, *Int. J. Biol. Macromol.*, 2025, **319**, 145475. https://doi.org/10.1016/j.ijbiomac.2025.145475

7 N. G. Khouri, J. O. Bahú, C. Blanco-Llamero, P. Severino, V. O. C. Concha, E. B. Souto, *J. Mol. Struct.*, 2024, **1309**, 138243. https://doi.org/10.1016/j.molstruc.2024.138243

8 M. Hussain, S. M. Khan, M. Shafiq, N. Abbas, *Giant*, 2024, **18**, 100261. https://doi.org/10.1016/j.giant.2024.100261

9 D. Merino, A. Zych, A. Athanassiou, *ACS Appl. Mater. Interfaces*, 2022, **14**, 46920–46931. https://doi.org/10.1021/acsami.2c10965

10 J. Tan, L. Cui, Z. Xie, Y. He, W. Dai, K. Xie, Y. Liu, *Chem. Eng. J.*, 2026, 537, 176327. https://doi.org/10.1016/j.cej.2026.176327

11 H. R. Dana, F. Ebrahimi, *Polym. Eng. Sci.*, 2023, **63**, 22–43. https://doi.org/10.1002/pen.26193

12 X. Wang, L. Huang, Y. Li, Y. Wang, X. Lu, Z. Wei, Q. Mo, S. Zhang, Y. Sheng, C. Huang, H. Zhao, Y. Liu, *J. Manuf. Process.*, 2024, **112**, 161–178. https://doi.org/10.1016/j.jmapro.2024.01.038

13 I. Plamadiala, C. Croitoru, M. A. Pop, I. C. Roata, *Polymers*, 2025, **17**, 191. https://doi.org/10.3390/polym17020191

14 N. Arora, S. Dua, V. K. Singh, S. Kumar Singh, T. Senthilkumar, *Mater. Today Commun.*, 2024, 40, 109617. https://doi.org/10.1016/j.mtcomm.2024.109617

15 M. M. Islam, N. Haque, D. Lau, M. Bhuiyan, B. K. Pramanik, *Chem. Eng. J.*, 2025, **522**, 167057. https://doi.org/10.1016/j.cej.2025.167057

16 C. Moretti, L. Hamelin, L. G. Jakobsen, M. H. Junginger, M. M. Steingrimsdottir, L. Høibye, L. Shen, *Resour. Conserv. Recycl.*, 2021, **169**, 105508. https://doi.org/10.1016/j.resconrec.2021.105508

17 M. R. Hasan, I. J. Davies, A. Pramanik, M. John, W. K. Biswas, *Sustain. Manuf. Serv. Econ.*, 2024, **3**, 100020. https://doi.org/10.1016/j.smse.2024.100020

18 R. Paiva, M. Aznar, M. Wrona, A. P. de Lima Batista, C. Nerín, S. A. Cruz, *ACS Appl. Polym. Mater.*, 2024, **6**, 12154−12163. https://doi.org/10.1021/acsapm.4c02230

19 ISO 5425:2023: *Specifications for use of poly(lactic acid) based filament in additive manufacturing applications*, 1st ed.; International Organization for Standardization, Geneva, Switzerland, 2023. https://www.iso.org/standard/81238.html

20 L. Lendvai, V. L. Bódi, M. Danko, P. S. Varbanov, S. K. Jakab, *Macromol. Mater. Eng.*, 2025; **311**, e00349. https://doi.org/10.1002/mame.202500349

21 F. Verceux, S. Grammatikos, *Polym. Test.*, 2025, **152**, 108982. https://doi.org/10.1016/j.polymertesting.2025.108982

22 V. C. Agbakoba, N. Webb, E. Jegede, R. Phillips, S. P. Hlangothi, M. J. John, *Macromol. Mater. Eng.*, 2024, **309**, 2300276. https://doi.org/10.1002/mame.202300276

23 T. M. McGuire, A. Buchard, C. Williams, *J. Am. Chem. Soc.*, 2023, **145**, 19840–19848. https://doi.org/10.1021/jacs.3c05863

24 H. Zhai, Y. Fang, S. Fan, W. Wu, T. Sun, W. Rao, J. Ding, L. Yu, *Green Chem.*, 2025, **27**, 15639–15653. https://doi.org/10.1039/d5gc04260g

25 S. Ellis, A. Buchard, T. Junkers, *Chem. Sci.*, 2025, **16**, 211–217. https://doi.org/10.1039/d4sc05891g

26 B. Öztürk, A. Balci, S. Alemdar, N. P. Bayramgil, *Polymer*, 2024, **315**, 127810. https://doi.org/10.1016/j.polymer.2024.127810

27 R. Zhang, S. Jia, J. Li, Y. Xu, H. Chen, X. Zhang, *ACS Sustain. Chem. Eng.*, 2025, **13**, 11226−11237. https://doi.org/10.1021/acssuschemeng.5c01154

28 R. Yang, G. Xu, B. Dong, H. Hou, Q. Wang, *Macromolecules*, 2022, **55**, 1726–1735. https://doi.org/10.1021/acs.macromol.1c02085

29 K. Kumari, V. Krishnan, *ACS Sustain. Chem. Eng.*, 2025, **13**, 17740−17752. https://doi.org/10.1021/acssuschemeng.5c02260

30 Q. Liu, R. Yang, B. Dong, H. Sun, G. Xu, Q. Wang, *Polym. Degrad. Stab.*, 2024, **222**, 110706. https://doi.org/10.1016/j.polymdegradstab.2024.110706

31 A. Salini, P. M. Gonnelli, C. Padoan, Y. Helali, J. Waeytens, S. Fusco, D. Cannella, *ACS Sustain. Chem. Eng.*, 2025, **13**, 20705−20716. https://doi.org/10.1021/acssuschemeng.5c06901

32 C. Murguiondo, M. G. de Lacoba, A. García-Miró, R. Routsi, A. Prieto, J. Barriuso, *Int. J. Biol. Macromol.*, 2025, **330**, 147822. https://doi.org/10.1016/j.ijbiomac.2025.147822

33 V. Tournier, S. Duquesne, F. Guillamot, H. Cramail, D. Taton, A. Marty, I. André, *Chem. Rev.*, 2023, **123**, 5612−5701. https://doi.org/10.1021/acs.chemrev.2c00644

34 F. A. Leibfarth, N. Moreno, A. P. Hawker, J. D. Shand, *J. Polym. Sci., Part A: Polym. Chem.*, 2012, **50**, 4814–4822. https://doi.org/10.1002/pola.26303

35 P. Majgaonkar, R. Hanich, F. Malz, R. Brüll, *Chem. Eng. J.*, 2021, **423**, 129952. https://doi.org/10.1016/j.cej.2021.129952

36 Y. Zhang, C. Zhu, H. Wang, Y. Qi, P. Sun, Q. Zhang, W. Jiang, *Chem. Eng. J.*, 2025, **522**, 167298. https://doi.org/10.1016/j.cej.2025.167298

37 S. Marullo, M. Silaco, F. D'Anna, *ACS Sustain. Chem. Eng.*, 2025, **13**, 20766−20775. https://doi.org/10.1021/acssuschemeng.5c08785

38 M. Edge, N. Yadav, A. Al Rida Hmayed, A. P. Dove, A. Brandolese, *ChemSusChem*, 2025, **18**, e202500420. https://doi.org/10.1002/cssc.202500420

39 S. Liu, L. Hu, J. Liu, Z. Zhang, H. Suo, Y. Qin, *Macromolecules*, 2024, **57**, 4662−4669. https://doi.org/10.1021/acs.macromol.4c00360

40 L. Shao, Y.-C. Chang, C. Hao, M. Fei, B. Zhao, B. J. Bliss, J. Zhang, *Green Chem.*, 2022, **24**, 8716–8724. https://doi.org/10.1039/d2gc01745h

41 K. Cheng, Y.-I. Hsu, H. Uyama, *Green Chem.*, 2025, **27**, 7620–7630. https://doi.org/10.1039/d5gc01068c

42 R. Mi, L. Zeng, M. Wang, S. Tian, J. Yan, S. Yu, M. Wang, D. Ma, *Angew. Chem. Int. Ed.*, 2023, **62**, e202304219. https://doi.org/10.1002/anie.202304219

43 Z.-X. Luo, G.-Q. Tian, S.-C. Chen, G. Wu, Y.-Z. Wang, *Macromolecules*, 2024, 57, 6828−6837. https://doi.org/10.1021/acs.macromol.4c01104

44 S. Russo, N. Ferrentino, F. Santulli, G. Paul, M. Lamberti, M. Mazzeo, V. Venditto, L. Marchese, D. Pappalardo, *ACS Sustain. Chem. Eng.*, 2025, **13**, 15331−15341. https://doi.org/10.1021/acssuschemeng.5c04557

45 S. Viamonte-Aristizábal, A. García-Sancho, F. M. A. Campos, J. A. Martínez-Lao, I. Fernández, *Eur. Polym. J.*, 2021, **161**, 110818. https://doi.org/10.1016/j.eurpolymj.2021.110818

46 C. Qu, X. Han, H. Wang, R. Wang, Y. Zhang, W. Sun, Z. Shi, Y. Wang, P. Yin, *ACS Sustain. Chem. Eng.*, 2025, **13**, 12496–12508. https://doi.org/10.1021/acssuschemeng.5c03502

47 L. Pedrini, C. Zappelli, S. J. Connon, *ACS Sustain. Chem. Eng.*, 2025, *13*, 1424–1430. https://doi.org/10.1021/acssuschemeng.4c08491

48 D. Rubeš, J. Vinklárek, Š. Podzimek, J. Honzíček, *RSC Adv.*, 2024, **14**, 8536–8547. https://doi.org/10.1039/d3ra08500g

49 T. Foltýn, J. Všetečka, R. Svoboda, Š. Podzimek, J. Vinklárek, J. Honzíček, *Macromolecules*, 2025, **58**, 10324−10335. https://doi.org/10.1021/acs.macromol.5c01600

50 D. Rubeš, J. Vinklárek, L. Prokůpek, Š. Podzimek, J. Honzíček, *J. Mater. Sci.*, 2023, **58**, 6203–6219. https://doi.org/10.1007/s10853-023-08407-5

View Article Online
DOI: 10.1039/D6SU00297H

51 T. Foltýn, E. Matušková, D. Rubeš, J. Vinklárek, M. Litecká, A. Krejčová, J. Honzíček, *Prog. Org. Coat.*, 2024, **192**, 108459. https://doi.org/10.1016/j.porgcoat.2024.108459
52 J. Všetečka, T. Foltýn, R. Svoboda, Š. Podzimek, J. Honzíček, *ACS Appl. Polym. Mater.*, 2026, **8**, 2328−2338. https://doi.org/10.1021/acsapm.5c04487

View Article Online
DOI: 10.1039/D6SU00297H

Data availability statement. The raw data required to reproduce these findings will be made available on request.